

Supplementary Information

Exploring π -Conjugated Triphenylamine–Cyano Derivatives as Cost-Effective Hole Transporting Materials in Perovskite Solar Cell

Swathi M,^a Rachel Chetri,^a Vygintas Jankauskas,^b Gediminas Kreiza,^c Kasparas Rakstys,^d Vytautas Getautis,^d and Ahipa T.N.^{a*}

^a Centre for Nano and Material Sciences, Jain (Deemed-to-be University), Jain Global Campus, Kanakapura, Bangalore, Karnataka, India – 562112

^b Institute of Chemical Physics, Vilnius University, Saulėtekio al. 3, 10257 Vilnius, Lithuania

^c Institute of Photonics and Nanotechnology, Vilnius University, Saulėtekio al. 3, 10257 Vilnius, Lithuania

^d Department of Organic Chemistry, Kaunas University of Technology, Radvilenu pl. 19, Kaunas 50254, Lithuania

*Corresponding Author email address: tn.ahipa@jainuniversity.ac.in

Table of Contents:

- 1. Experimental Section**
 - 1.1 Materials and Methods**
 - 1.2 Solubility**
 - 1.3 Estimated Cost**
- 2. Analytical Data**
 - 2.1 ATR-IR Spectra**
 - 2.2 ¹H NMR and ¹³C NMR Spectra**
 - 2.3 Mass Spectra**
 - 2.4 Crystal Analysis Data**
 - 2.5 Photographic Images**
 - 2.6 FE-SEM**
 - 2.7 Contact Angle**
 - 2.8 Cyclic Voltammetry**
 - 2.9 Energy Gap Calculations**
 - 2.10 Charge Transporting Properties**
 - 2.11 Computational Details**
 - 2.12 Output Files**
- 3. References**

1. Experimental Section

Materials and Methods: 4-(*N,N*-Diphenylamino)benzaldehyde was purchased from BLD Pharmatech (India) Pvt Ltd, while S D Fine Chem Ltd. supplied potassium carbonate, ammonium acetate, and ethylcyanoacetate. Further, *N,N*-dimethylformamide, 1-bromobutane, 1,4-dioxane, and 4-acetylbenzonitrile were purchased from Avra Synthesis Pvt. Ltd. Telangana, India, and the solvents were purchased from Rankem Chemicals. On a ZnSe crystal, IR spectra were obtained using a Bruker ALPHA eco-ATR-IR. With DMSO-*d*₆/CDCl₃ as the solvent and TMS as the internal standard, 400 MHz JEOL NMR spectrometer was used to obtain the ¹H and ¹³C NMR spectra. An e2695/HPLC-TQD mass spectrometer from Water Alliance provided the ESI-MS. The RF-5301 PC, SHIMADZU spectrophotometer with a Xe-lamp as an excitation source and the UV-1800 SHIMADZU UV-spectrophotometer were used to measure the emission and UV-visible absorption characteristics, respectively.

Electrochemical measurements were carried out in an electrochemical workstation, CH instrument Model 750E, on a glassy carbon electrode. The thin films were coated in the Plaslabs, US N₂ dry glove box and Spin-NXG-P1 spin coating machine. The glass plates were cleaned using acetone in ultra-sonicator and dried in an oven. The substrates were then cleaned by UV-ozone treatment and kept in a nitrogen environment along with samples. The solutions were then coated on the glass slides by spin-coating in a glove box at 3000 rpm for 40 seconds by keeping the quantity of solution taken for coating as a constant. The TGA Q500 V20.10 Build 36 instrument under N₂ gas atmosphere at a heating rate of 10 °C/min was utilized for the TGA and DSC analysis. A TECH contact angle measurement instrument (Model No: TECH CON- 1200) was used for the contact angle measurements. The photographic images of the crystals were taken from an Olympus BX53M microscope, and the obtained images were processed using PRECiV Core software. After being chosen under a microscope, the appropriate single crystal was placed on a microloop (MiTeGen) using inert oil and examined at 100.0 K using an XtaLab Synergy (Rigaku) diffractometer fitted with a HyPix-6000HE detector and a PhotonJet X-ray source (CuK α , λ = 1.54184). CrysAlisPro software was used to gather data and S-3 process. Using Least Squares minimization as implemented in the Olex2 graphical interface,¹ the structures were polished with the ShelXL² package after being solved by

Intrinsic Phasing with the ShelXT³ software. JEOL (Model-JSM7100F) was used for the FE-SEM analysis.

1.2 Solubility

Table S1: Solubility limits of TPA-CN and TPA-CNA in different solvents.

Solvent	Solubility Limit (mg/mL)	
	TPA-CN	TPA-CNA
Dimethyl sulphoxide	30 mg/mL	5 mg/mL
<i>N,N</i> -Dimethylformamide	70 mg/mL	30 mg/mL
Ethyl acetate	Insoluble	7.5 mg/mL
Tetrahydrofuran	8 mg/mL	80 mg/mL
Dichloromethane	4 mg/mL	40 mg/mL
Chloroform	1 mg/mL	>125 mg/mL
Diethyl ether	Insoluble	1 mg/mL
Chlorobenzene	Insoluble	80 mg/mL
Toluene	Insoluble	30 mg/mL
Hexane	Insoluble	Insoluble

1.3 Estimated Cost

Table S2: Cost calculation of TPA-CN.

Chemicals	Vendor	Weight of reagent (g)	Price (Rs)	Amount required (g)	Price (Rs)
4-(<i>N,N</i> -diphenylamino)benzal dehyde	BLD Pharmatech (India) Pvt. Ltd.	25	3669	2	293.52
4-acetylbenzonitrile	Avra synthesis Pvt. Ltd.	25	4301	1.06	182.36
Ethylcyanoacetate	S D Fine Chem Ltd	500 ml	814	935 µl	1.52
Ammonium acetate	S D Fine Chem Ltd	500	511	4.51	4.61
1,4-dioxane	Avra synthesis Pvt. Ltd.	500 ml	933	20 ml	37.32
Total Cost	519.33				
Amount of TPA-CN	1.475 g				
Total cost of TPA-CN	352.09 (Rs) or 4.02 (\$)*				

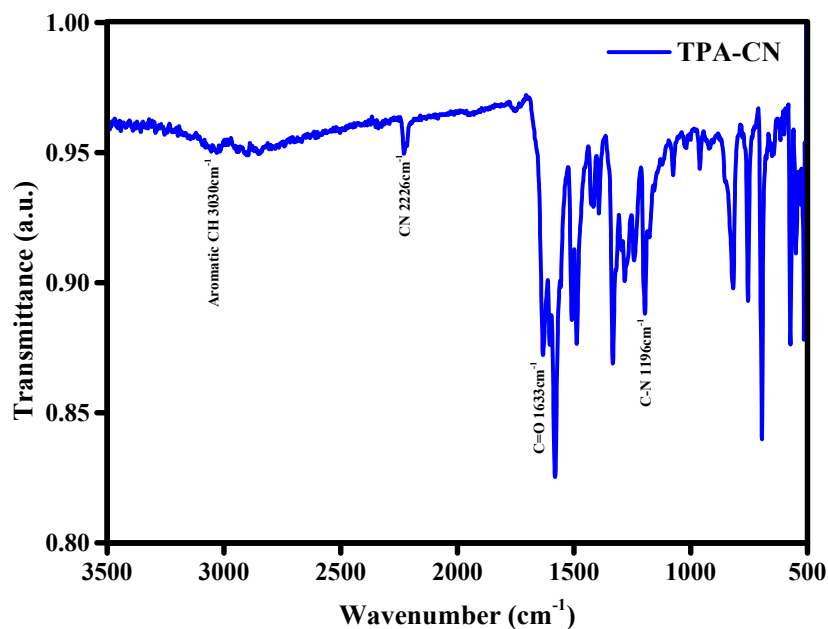
Table S3: Cost calculation of TPA-CNA.

Chemicals	Vendor	Weight of reagent (g)	Price (Rs)	Amount required (mg)	Price (Rs)
TPA-CN	Lab synthesis	1	352.09	2.25	792.19
1-bromobutane	Avra synthesis Pvt. Ltd.	100 ml	472	348.25 μ l	1.64
Potassium Carbonate	S D Fine Chem Ltd	500	459	501.98	0.46
<i>N,N</i> -dimethylformamide	Avra synthesis Pvt. Ltd.	2500 ml	1600	5 ml	3.2
Total cost	797.49				
Amount of TPA-CNA	1 g				
Total cost of TPA-CNA	797.49 (Rs) or 9.11 (\$)*				

*1 INR = 0.011 USD is the conversion factor used.

2. Analytical Data

2.1 ATR-IR Spectra

**Fig. S1:** ATR-IR Spectra of TPA-CN.

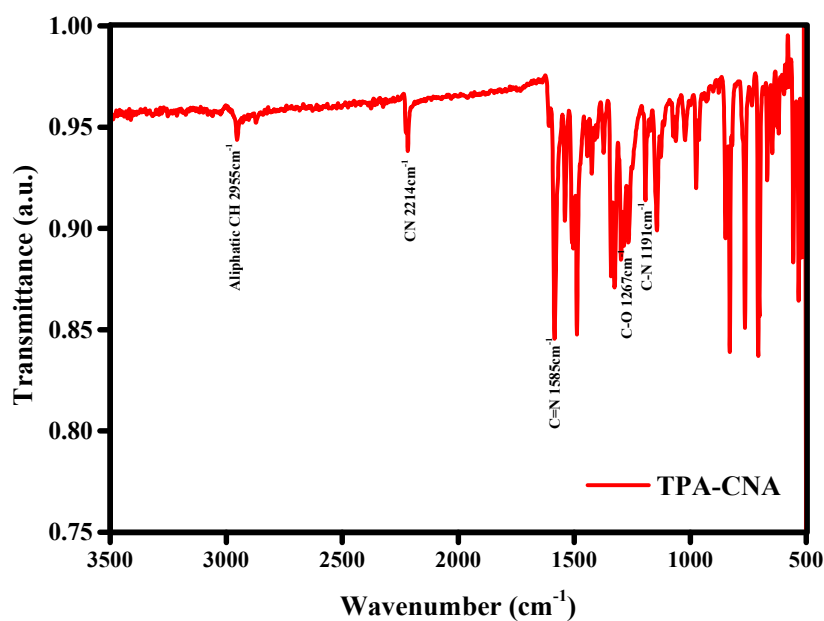


Fig. S2: ATR-IR Spectra of TPA-CNA.

For the interaction studies, HTMs and the mixture of HTM and PbI₂ (1:2 mole/mole ratio) were stirred in THF for an hour. After the complete evaporation of solvent, the residual solids are then used for the analysis.⁴

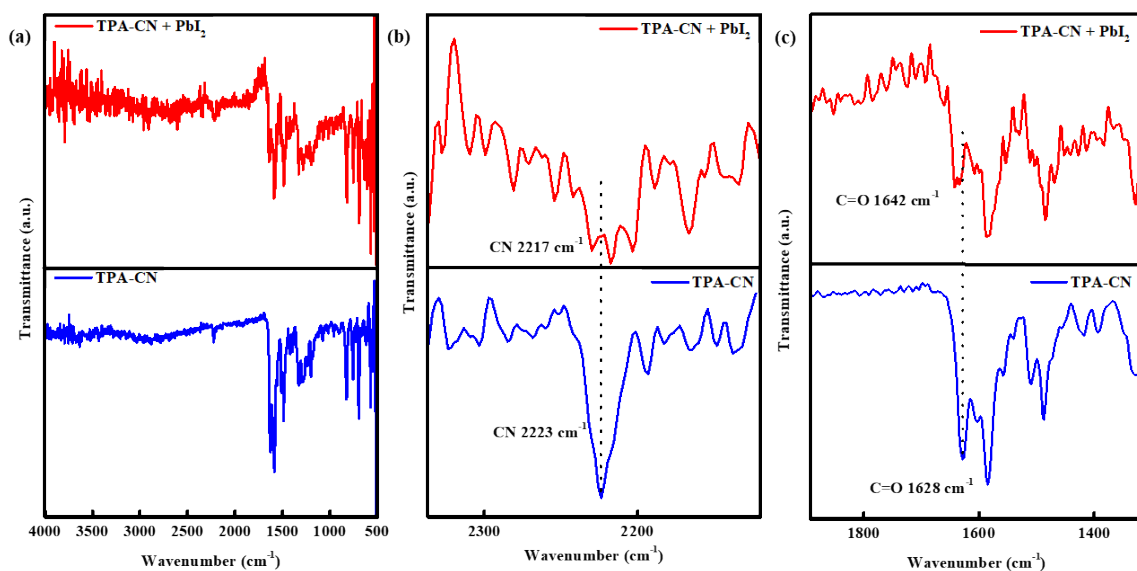


Fig. S3: (a) ATR-IR spectra of TPA-CN and TPA-CN + PbI₂. (b) CN band of TPA-CN and TPA-CN + PbI₂. (c) C=O band of TPA-CN and TPA-CN + PbI₂.

TPA-CN: ^1H NMR (400 MHz, $\text{DMSO}-d_6$), δ (ppm): 12.63 (s, 1H), 8.01 (dd, $J = 3.8, 1.1$ Hz, 1H), 7.84 (s, 1H), 7.68 – 7.53 (m, 2H), 7.43 – 7.31 (m, 5H), 7.25 – 7.18 (m, 1H), 7.17 – 7.06 (m, 7H), 6.96 (d, $J = 8.7$ Hz, 2H). (**Fig. S4**)

TPA-CNA: ¹H NMR (400 MHz, CDCl₃), δ (ppm): 8.20 – 8.13 (m, 2H), 7.80 – 7.73 (m, 2H), 7.55 – 7.50 (m, 2H), 7.46 (s, 1H), 7.35 – 7.27 (m, 4H), 7.19 – 7.15 (m, 4H), 7.14 – 7.08 (m, 4H), 4.57 (t, J = 6.6 Hz, 2H), 1.88 (dt, J = 14.4, 6.6 Hz, 2H), 1.60 – 1.52 (m, 2H), 1.01 (t, J = 7.4 Hz, 3H). (**Fig. S6**)

¹³C NMR (100 MHz, CDCl₃), δ (ppm): 165.29, 156.62, 155.29, 149.99, 146.91, 141.81, 132.69, 129.67, 129.43, 128.18, 127.83, 125.67, 124.29, 121.52, 112.73, 93.91, 67.60, 30.94, 19.35, 13.99. (**Fig. S7**)

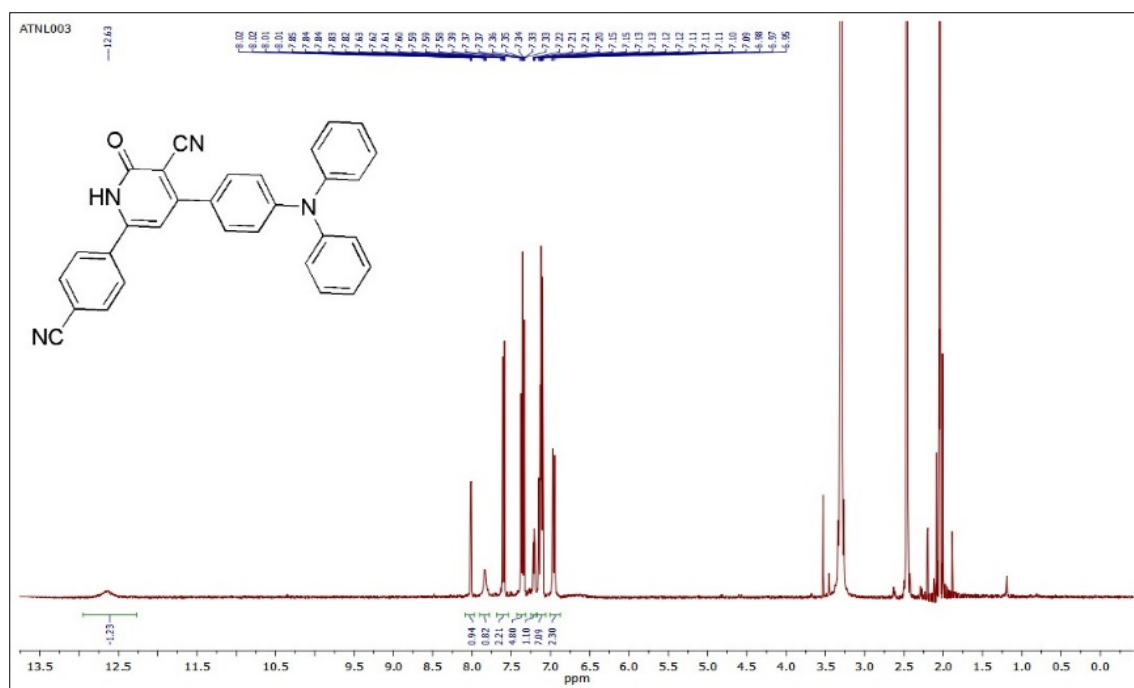


Fig. S4: ^1H NMR of TPA-CN recorded in DMSO- d_6 .

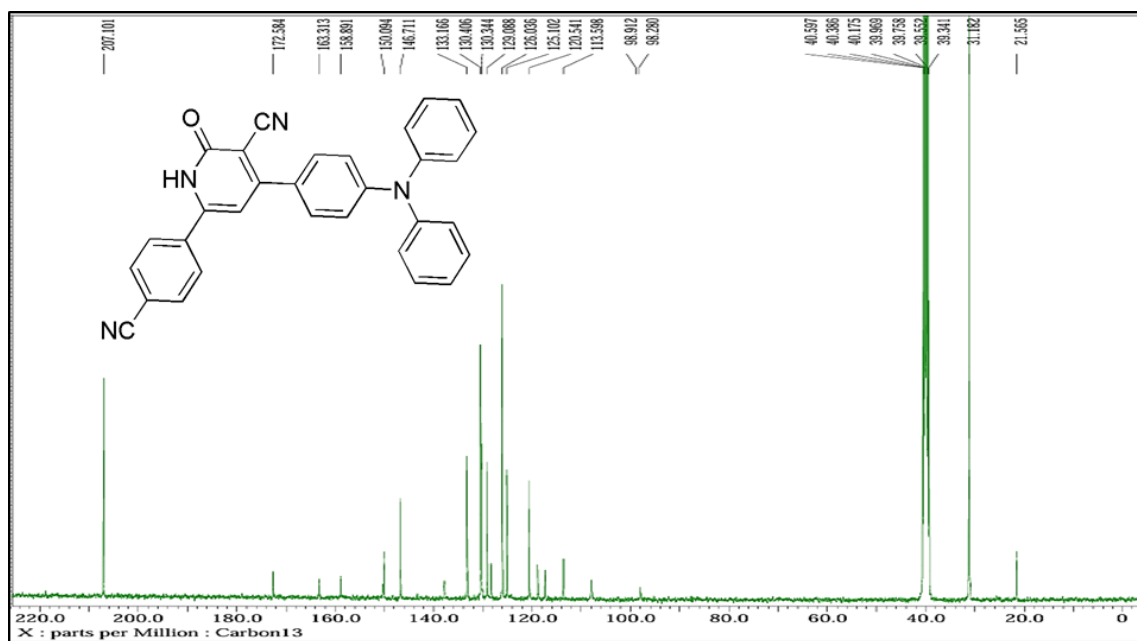


Fig. S5: ^{13}C NMR of TPA-CN recorded in DMSO- d_6 .

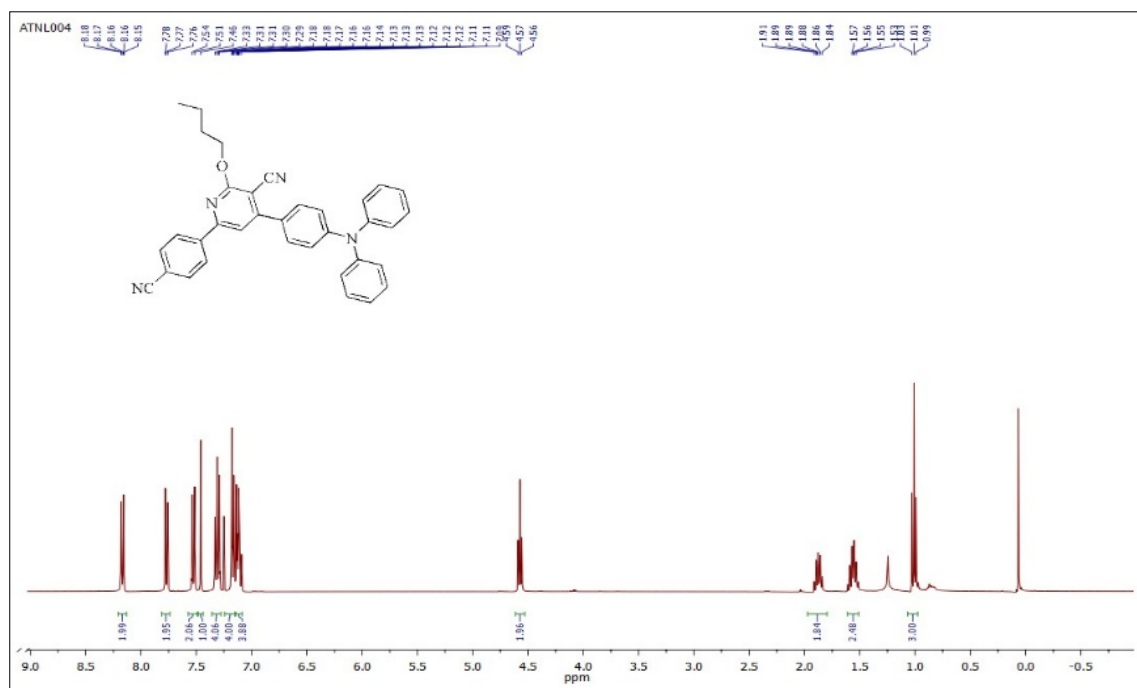


Fig. S6: ^1H NMR of TPA-CNA recorded in CDCl_3 .

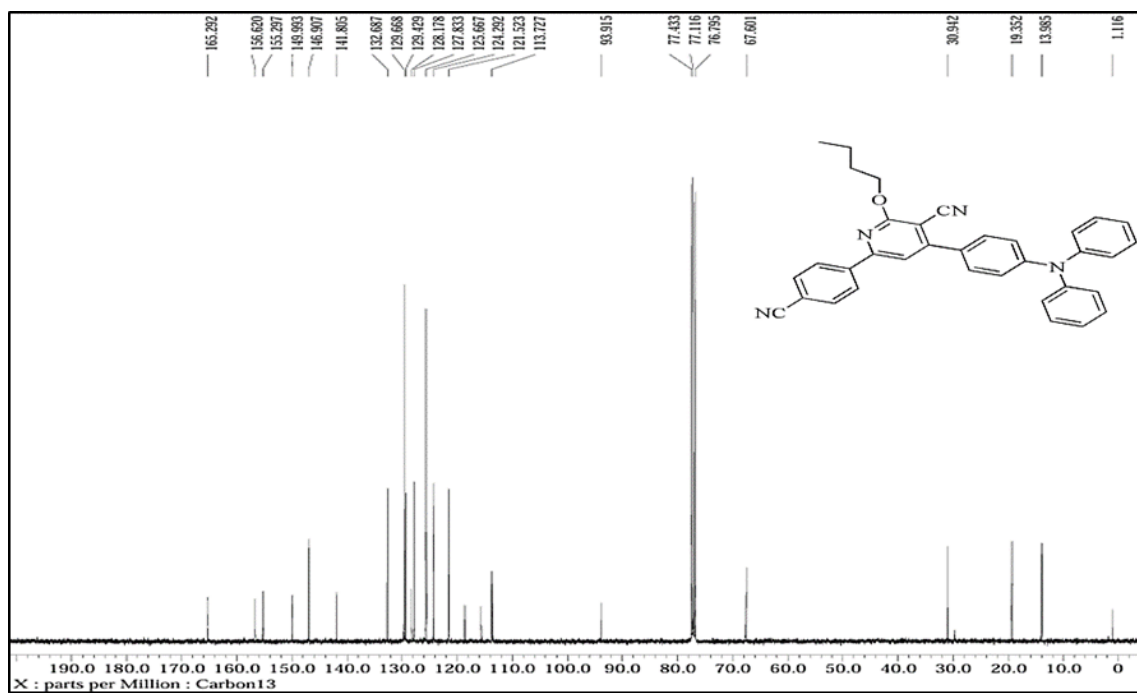


Fig. S7: ¹³C NMR of TPA-CNA recorded in CDCl₃.

2.3 Mass Spectra

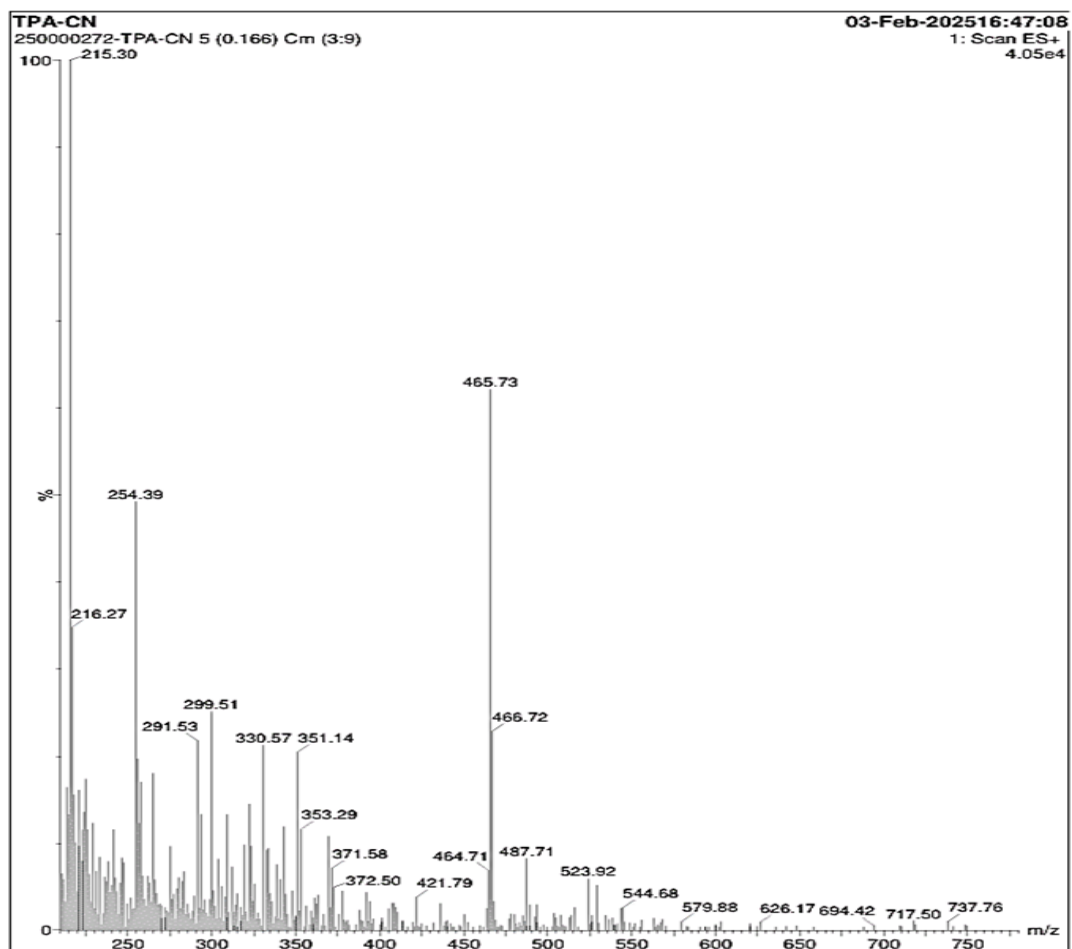


Fig. S8: Mass spectrum of TPA-CN.

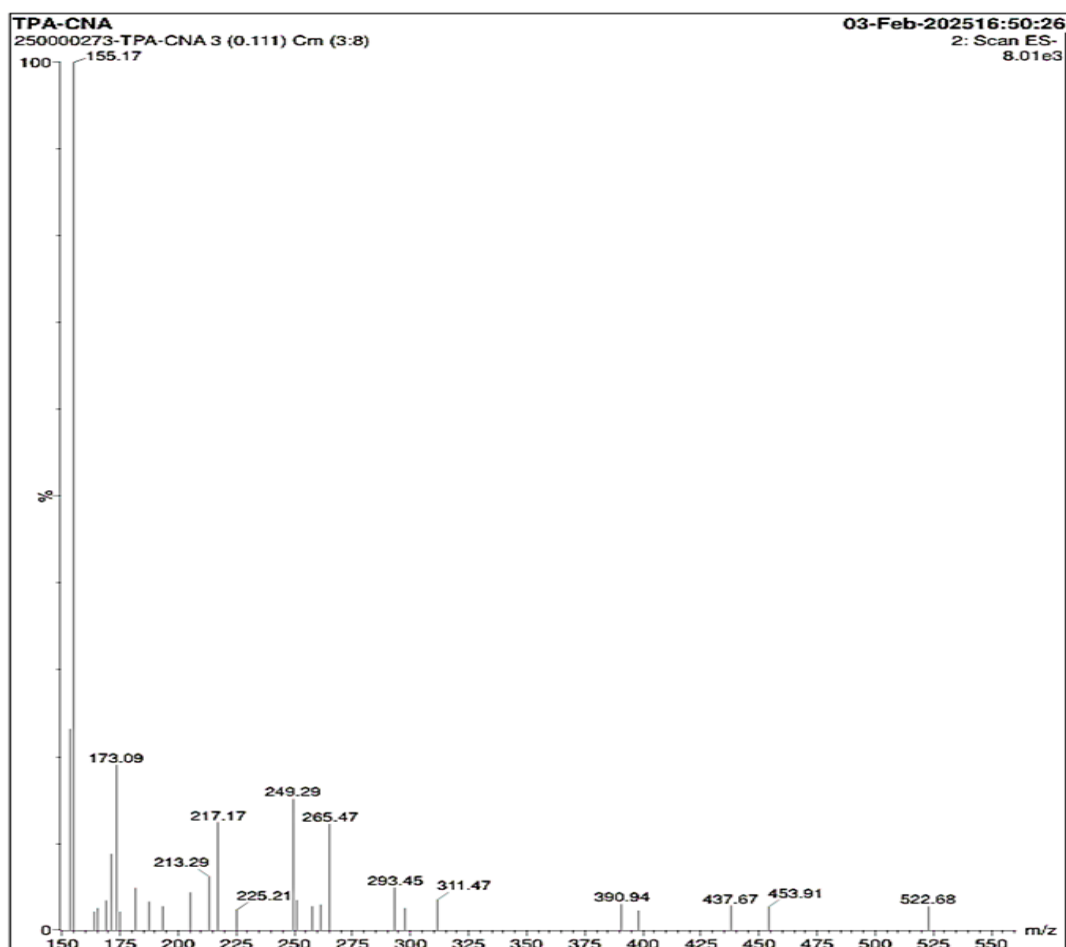


Fig. S9: Mass spectrum of TPA-CNA.

2.4 Single Crystal Analysis

Single crystals of the samples were grown using slow evaporation of the samples in THF (TPA-CN – CCDC No: **2484579**) and Ethyl acetate (TPA-CNA – CCDC No: **2484580**) solvents and analysed using X-ray crystallography. The photographic images of the crystals under microscope in 20X magnification are given in **Fig. S9**.

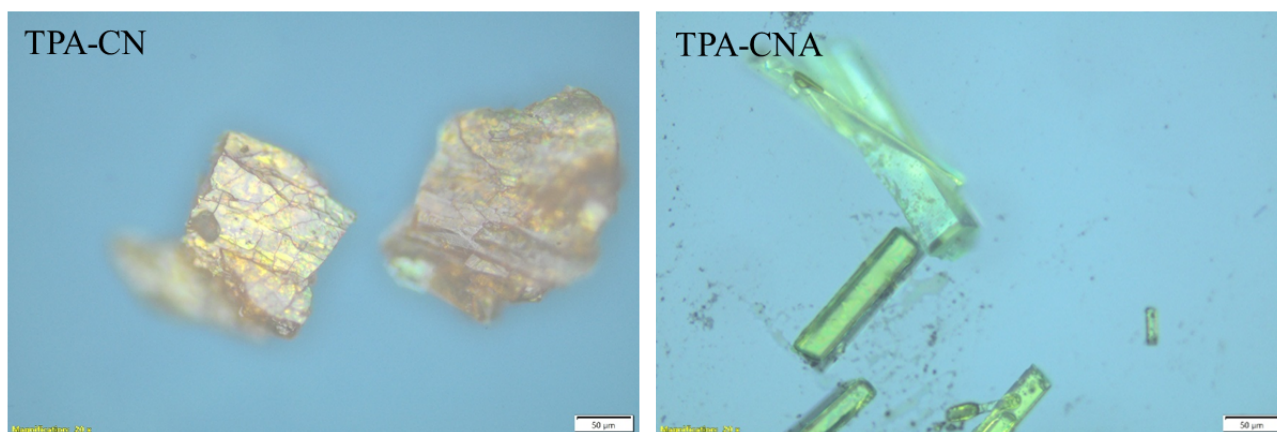


Fig. S10: Photographic images of the crystals under optical microscope.

Table S4: Crystallographic parameters of **TPA-CN** and **TPA-CNA**.

	TPA-CN	TPA-CNA
Empirical formula	C ₃₁ H ₂₀ N ₄ O, C ₄ H ₈ O	C ₃₅ H ₂₈ N ₄ O
Formula weight (<i>g/mol</i>)	536.61	520.61
Temperature, <i>K</i>	296	297
Crystal system	Triclinic	Monoclinic
<i>a</i> , Å	10.8462	13.6359
<i>b</i> , Å	11.5602	8.1690
<i>c</i> , Å	12.1304	26.2883
<i>α</i> , deg	80.864	90
<i>β</i> , deg	75.689	103.490
<i>γ</i> , deg	74.009	90
<i>V</i> , Å ³	1410.01	2847.51
Space group	<i>P</i> $\bar{1}$	P2 ₁ /c
Z value	2	4
ρ_{calc} , g/cm ³	1.264	1.214
μ , mm ⁻¹	0.633	0.584
F (000)	564.0	1096.0
Radiation	CuK α (λ = 1.54184)	CuK α (λ = 1.54184)

Table S5: Short contacts of **TPA-CN**.

Number	Object 1	Object 2	Length (Å)
1	HM	HM	2.160
2	O34	N6	2.792
3	O34	H	1.948
4	O34	C12	3.159
5	O34	HA	2.426
6	N14	HO	2.714
7	N36	H40B	2.593
8	HC	O39	2.691

Table S6: Short contacts of TPA-CNA.

Number	Object 1	Object 2	Length (Å)
1	H9	N33	2.674
2	C29	H19	2.892
3	C30	H19	2.869
4	H31	N39	2.670
5	C32	H18	2.796

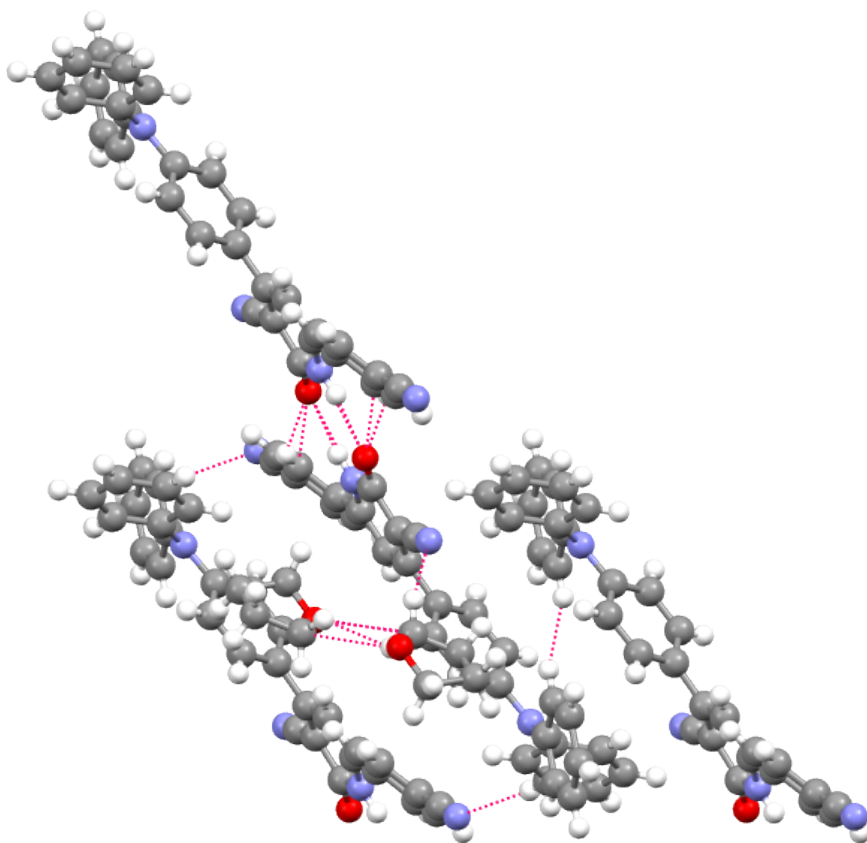


Fig. S11: Short contacts of TPA-CN (dashed pink lines) as viewed from the 'a' axis.

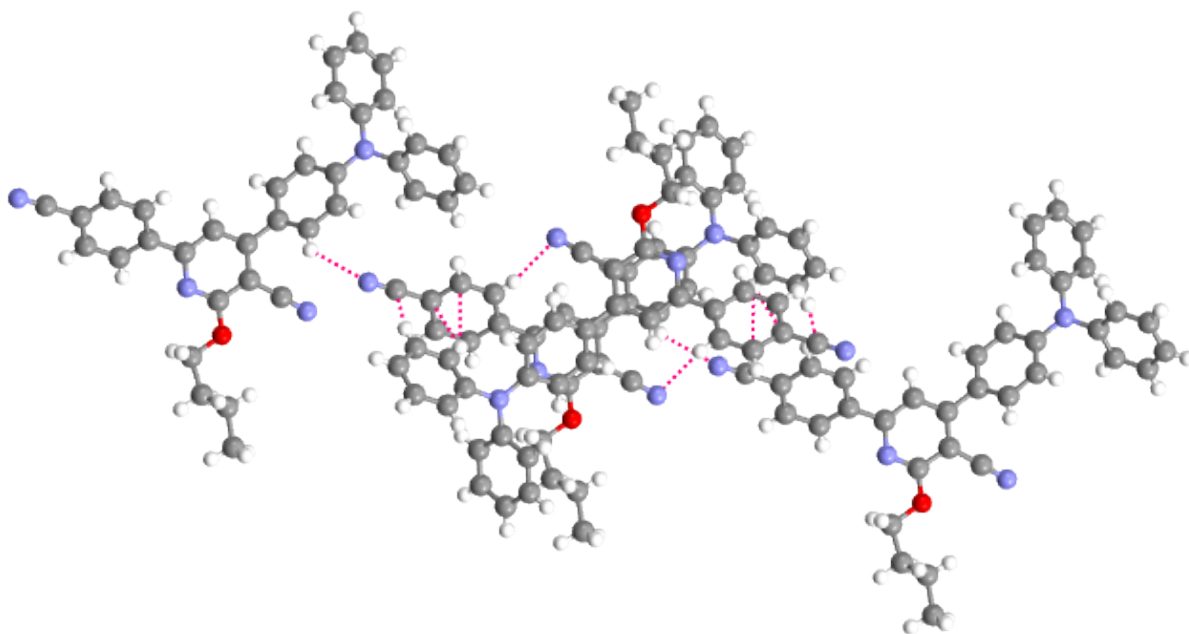


Fig. S12: Short contacts of **TPA-CNA** (dashed pink lines) as viewed from the ‘b’ axis.

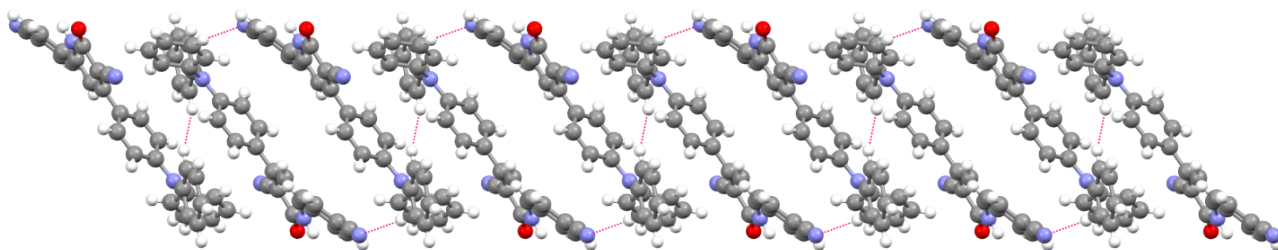


Fig. S13: View down the ‘a’ axis of the stacking **TPA-CN** molecules (dashed pink lines indicate short contacts).

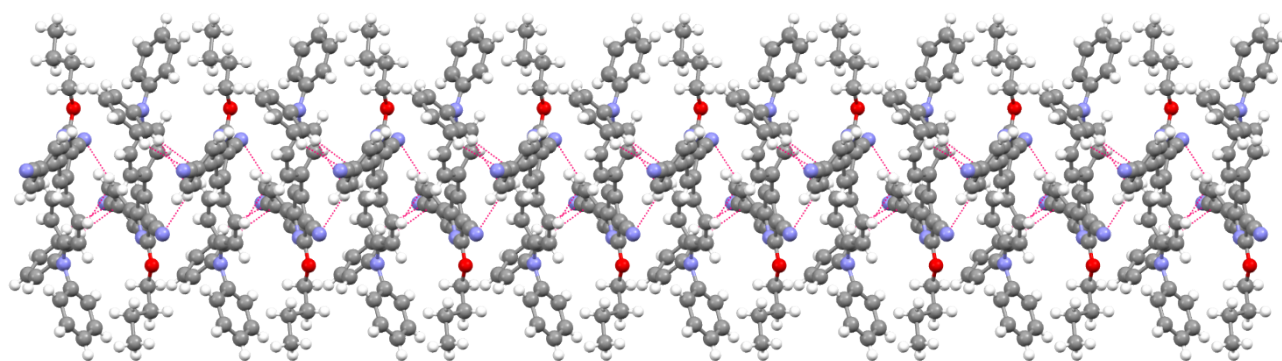


Fig. S14: View down the ‘a’ axis of the stacking TPA-CNA molecules (dashed pink lines indicate short contacts).

2.5 Photographic Images

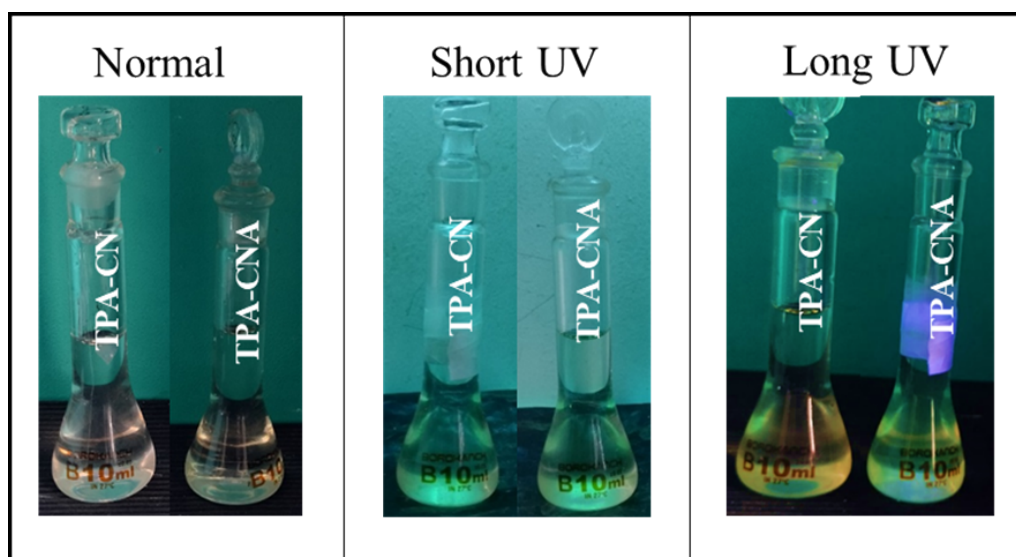


Fig. S15: Photographic image of TPA-CN and TPA-CNA in 10^{-5} M DMSO solution taken under normal light, short UV and long UV light illuminations.

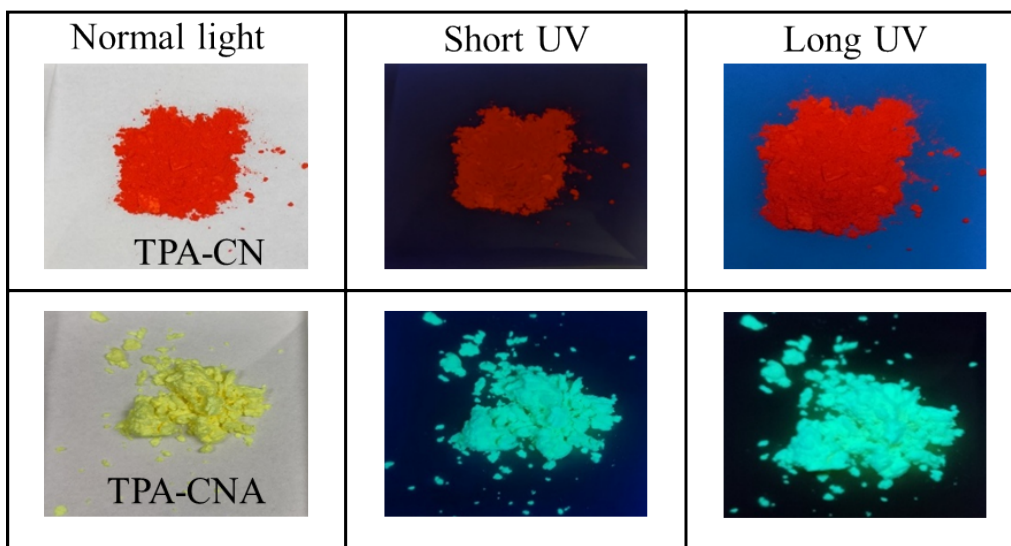


Fig. S16: Photographic images of **TPA-CN** and **TPA-CNA** solid samples taken under normal light, short UV and long UV illuminations.

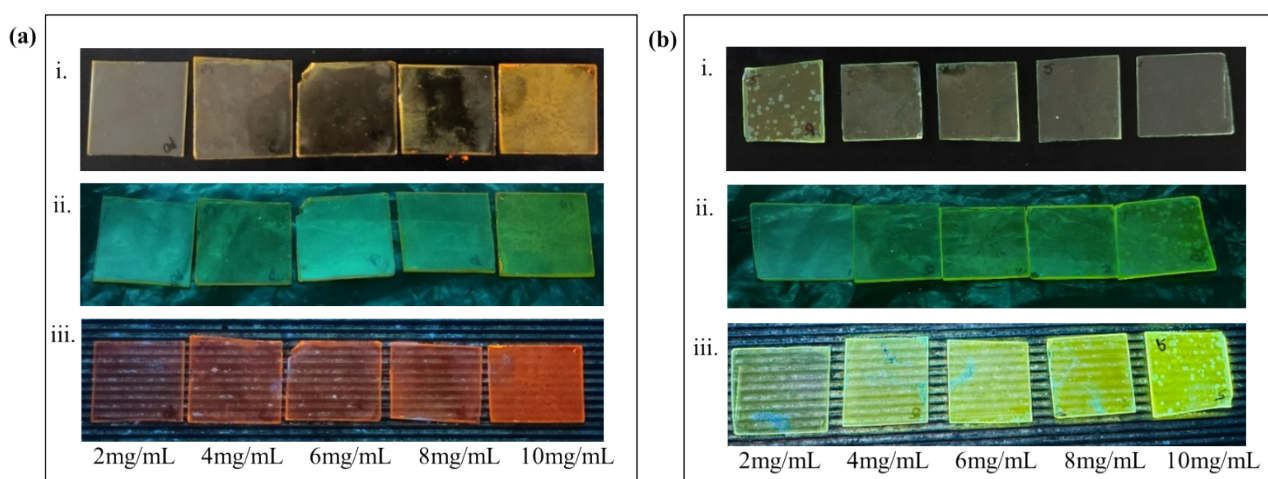


Fig. S17: Photographic images of thin films of **(a) TPA-CN** and **(b) TPA-CNA** under (i) Normal Light; (ii) Short UV Light and (iii) Long UV Light.

2.6 FE-SEM

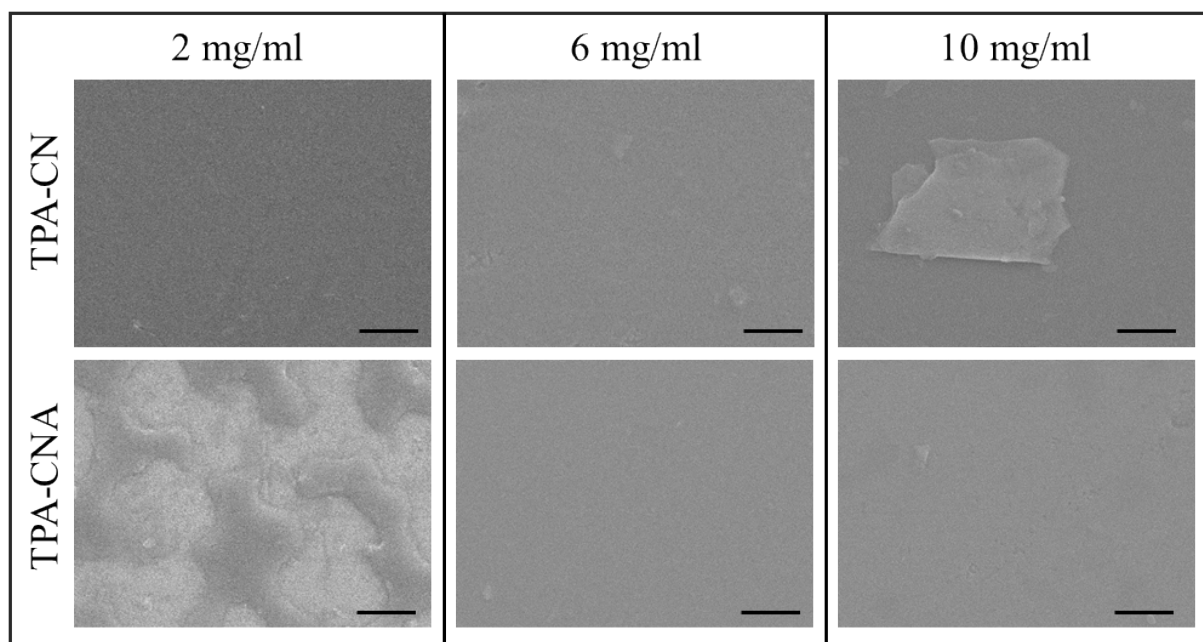
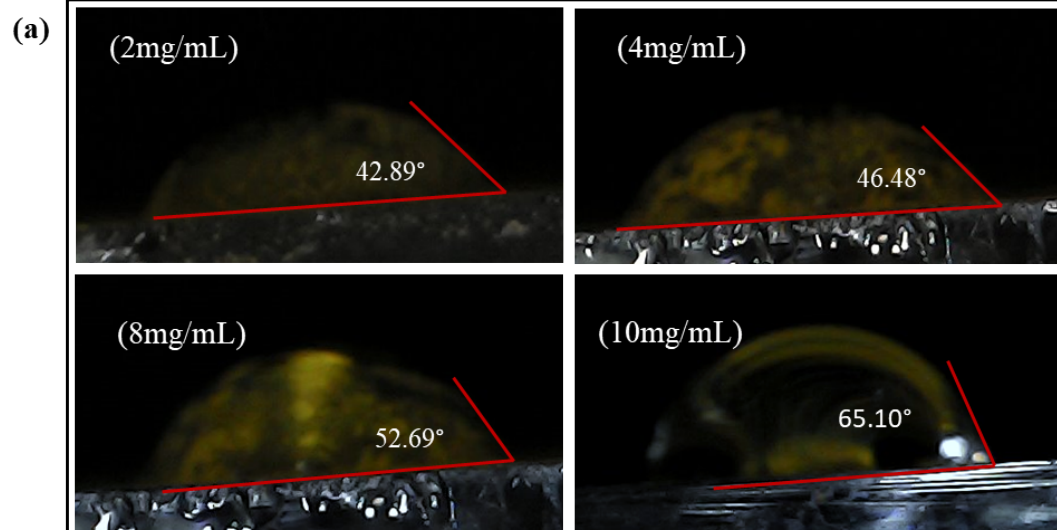


Fig. S18: FE-SEM images of **TPA-CN** and **TPA-CNA** in thin films of different concentration (The line insert indicates 1 μm).

2.7 Contact Angle



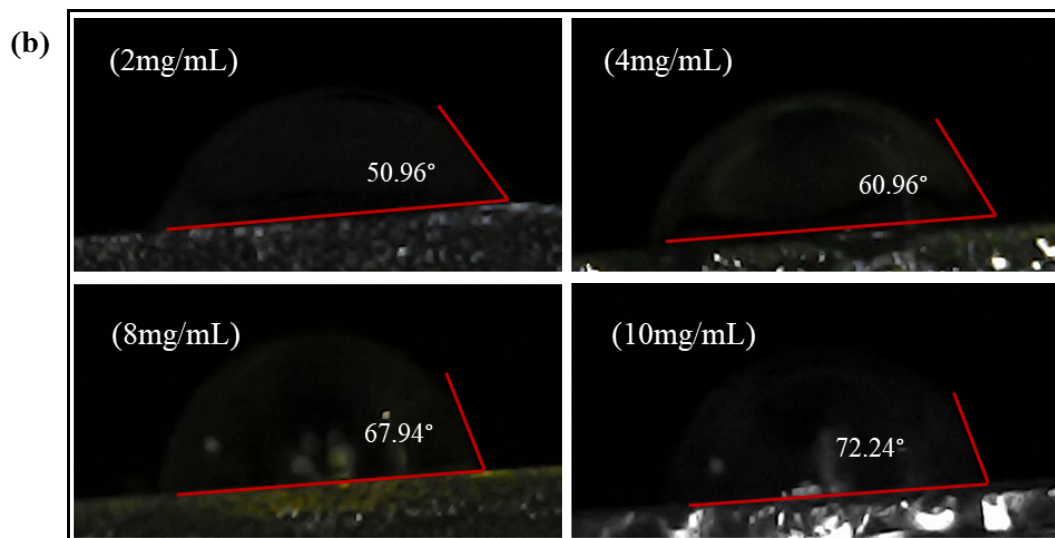


Fig. S19: Contact angle measurements of (a) TPA-CN and (b) TPA-CNA drop casted films.

2.8 Cyclic Voltammetry

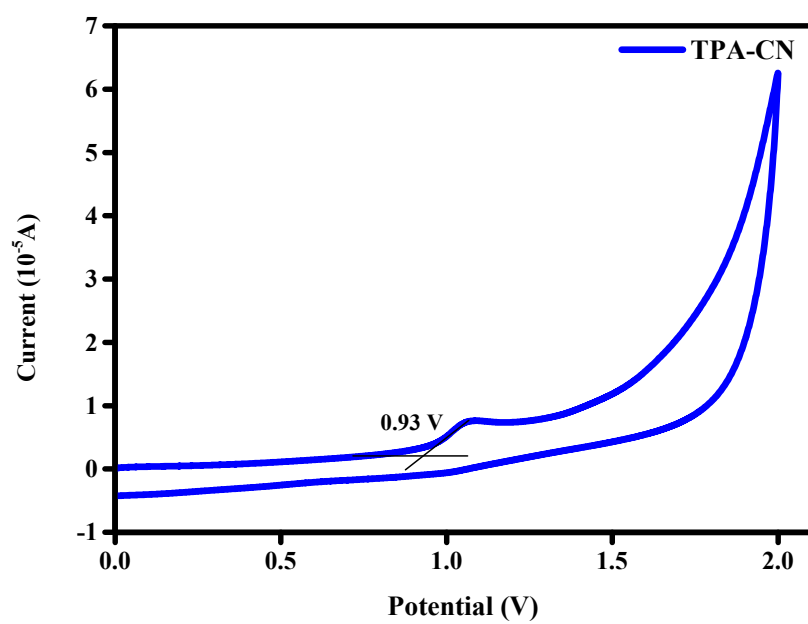


Fig. S20: Cyclic Voltammogram of TPA-CN.

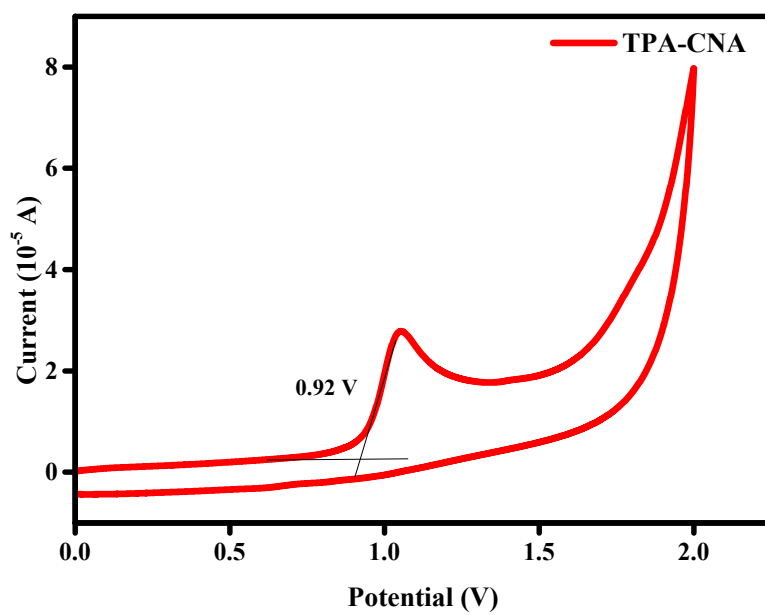


Fig. S21: Cyclic Voltammogram of TPA-CNA.

2.9 Calculations

TPA-CN

$$E_g \text{ (eV)} = 1240/\lambda_{\text{int}}$$

$$\lambda_{\text{int}} = \mathbf{456 \text{ nm}}$$

$$\begin{aligned} E_g &= 1240/445 \\ &= \mathbf{2.72 \text{ eV}} \end{aligned}$$

$$\begin{aligned} E_{\text{HOMO}} &= -4.78 + [E_{\text{OX}}(\text{Fc}) - E_{\text{OX}}] \\ &= -4.78 + (0.4076 - 0.93) \\ &= \mathbf{-5.30 \text{ eV}} \end{aligned}$$

Where, $E_{\text{OX}}(\text{Fc}) = 0.4076$

$$\begin{aligned} E_{\text{LUMO}} &= E_g + E_{\text{HOMO}} \\ &= 2.72 - 5.30 \\ &= \mathbf{-2.58 \text{ eV}} \end{aligned}$$

TPA-CNA

$$E_g \text{ (eV)} = 1240/\lambda_{\text{int}}$$

$$\lambda_{\text{int}} = \mathbf{434 \text{ nm}}$$

$$\begin{aligned} E_g &= 1240/434 \\ &= \mathbf{2.86 \text{ eV}} \end{aligned}$$

$$\begin{aligned} E_{\text{HOMO}} &= -4.78 + [E_{\text{OX}}(\text{Fc}) - E_{\text{OX}}] \\ &= -4.78 + (0.4076 - 0.92) \\ &= \mathbf{-5.29 \text{ eV}} \end{aligned}$$

Where, $E_{\text{OX}}(\text{Fc}) = 0.4076$

$$\begin{aligned} E_{\text{LUMO}} &= E_g + E_{\text{HOMO}} \\ &= 2.86 - 5.29 \\ &= \mathbf{-2.43 \text{ eV}} \end{aligned}$$

2.10 Charge Transporting Properties

To describe charge transport in compound films, the xerographic time-of-flight (XTOF) technique was employed. Drop casting is used to create samples on Al-coated glass plates using THF (**TPA-CNA**) and DMSO (**TPA-CN**). The sample was 1-3.2 μm thick. The sample crystallized after the solvent dried, despite **TPA-CN** dissolving in THF solvent as well, however, the solubility was insufficient. The substance **TPA-CN** also tried to crystallize with DMSO, but drying on a hotplate set at 80 $^{\circ}\text{C}$ stopped it. The THF solvent produced a flawlessly constructed **TPA-CNA** sample. In the XTOF analysis, the **TPA-CN** sample's quality was simply inadequate and shown minimal electrification.

The electric field in the sample is produced by corona charging. Nitrogen laser pulses with a wavelength of 337 nm and a duration of 1 ns were used to illuminate the layer surface, creating charge carriers. About 10% of the initial potential was lost as a result of the layer surface potential due to pulse lighting. The rate at which the surface potential decreased, dU/dt , was measured by the capacitance probe that was placed over the sample and coupled to the wide frequency band electrometer. The kink on the double logarithmic scale dU/dt transient curve was used to calculate the transit time t_t . Dispersive charge transport is a characteristic of these materials. Using the formula $d^2/U_0 t_t$, where d is the

layer thickness and U_0 is the surface potential at illumination, the drift mobility was determined. The usual plot for organic compounds displays the mobility data for holes and electrons.

2.11 Computational Details

The Gaussian 09 software program was used for all of the calculations in this investigation. Using the B3LYP hybrid functional at 6-311G(d) basis set in conjunction with density functional theory (DFT), the ground state geometry optimizations of the planned molecules were thoroughly simulated. To gain understanding of the structures and associated electro-optical properties, the band gap energies and frontier molecular orbitals (FMOs), such as HOMOs and LUMOs, were examined. To study the electronic characteristics such the ionization potential (IP) and electron affinity (EA), the energies of neutral, cationic, and anionic states were ascertained. Using time dependent DFT (TD-DFT) at the B3LYP/CAM-B3LYP/ ω B97XD level of theory and a basis set of 6-311G(d), the optical properties, including the maximum absorption wavelengths (λ_{max}), were calculated based on the optimized geometries. TDM maps that were created with Multiwfn and are used to examine the electron-hole coherence correlation of charge transfer based on electronic transitions.^{5, 6} To further clarify the charge transfer characteristics, simulations of the hole transport rate and electron and hole reorganization energy using Marcus theory have been conducted.

IR Spectra:

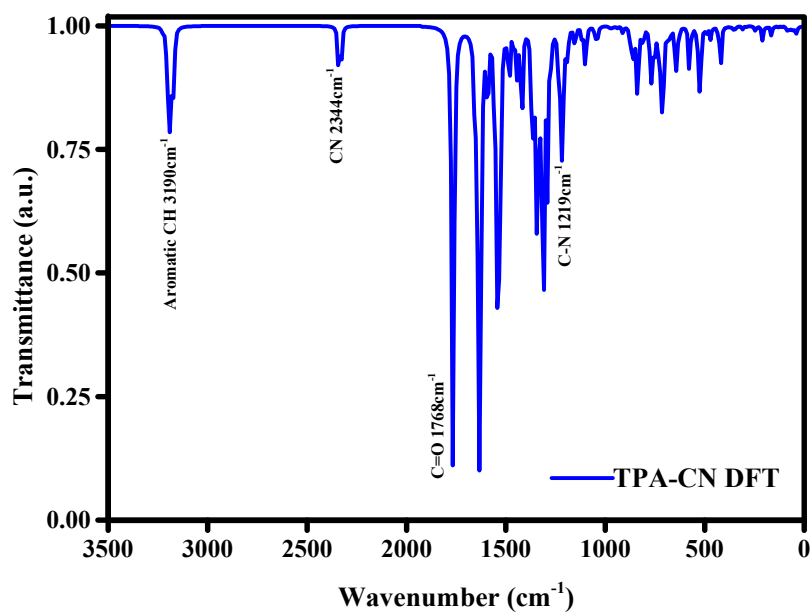


Fig. S22: IR spectra of TPA-CN predicted using B3LYP/6-311G(d) level of theory.

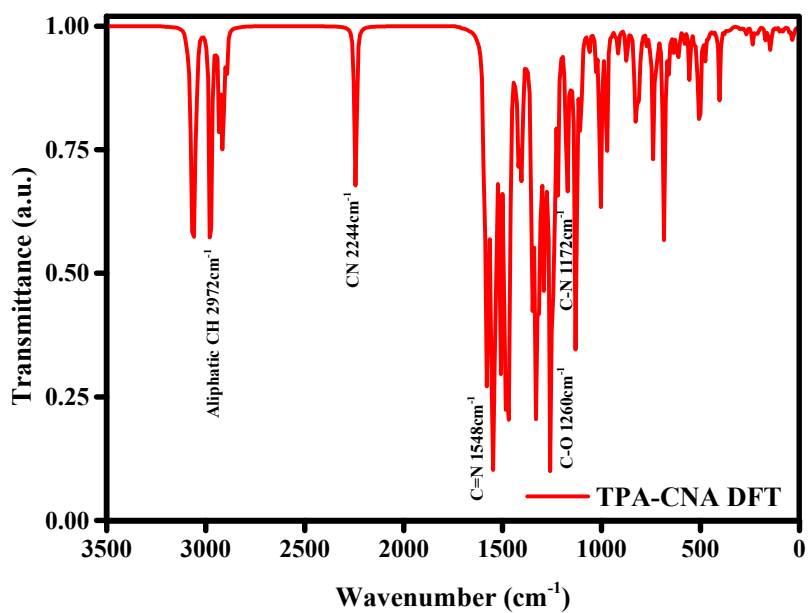


Fig. S23: IR spectra of TPA-CNA predicted using B3LYP/6-311G(d) level of theory.

Absorption Spectra

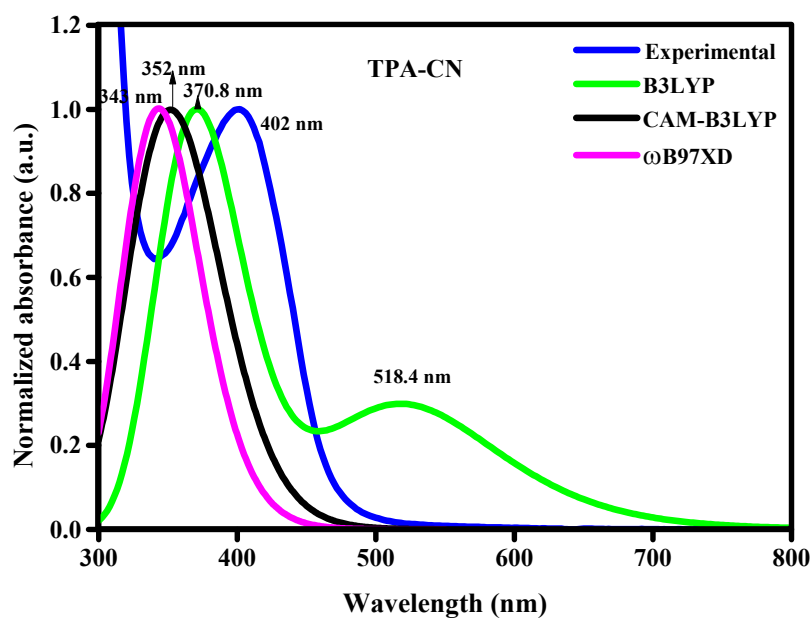


Fig. S24: Comparison of experimental and simulated absorption values of TPA-CN and (using TD-DFT/ B3LYP/ CAM-B3LYP/ ω B97XD/ CPCM (DMSO) level of theory.

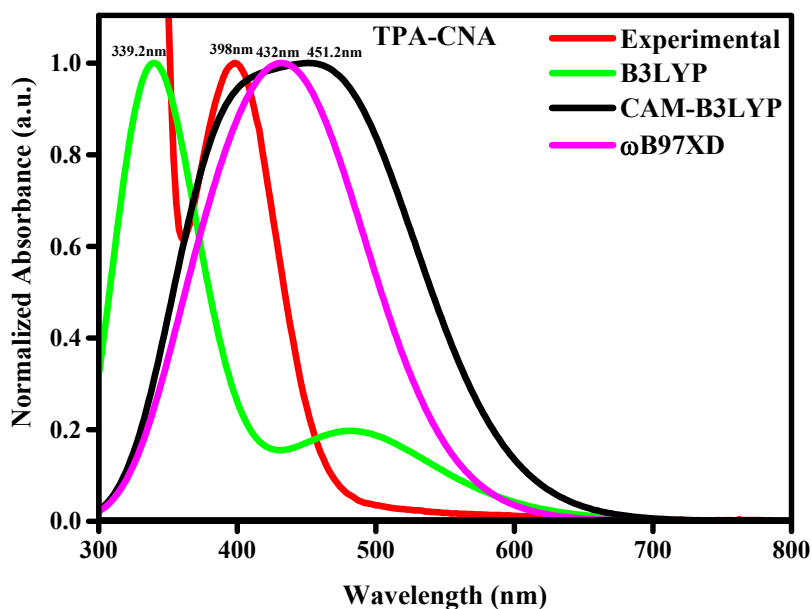


Fig. S25: Comparison of experimental and simulated absorption values of TPA-CNA and (using TD-DFT/ B3LYP/ CAM-B3LYP/ ω B97XD/ CPCM (DMSO) level of theory.

2.12 Output Files

Output file of **TPA-CN** (B3LYP/6-311G(d))

C	-3.26394322	0.32338568	-1.17464724
C	-0.98395022	1.64983493	-0.40062208
C	-2.20996797	2.01687050	0.16599626
C	-3.34285061	1.34214899	-0.20601344
H	-4.28072028	1.60769764	0.23479387
C	-4.55829381	-0.45016025	-1.58171143
C	-4.52305057	-1.44487936	-2.53762250
C	-5.77343569	-0.12122108	-0.97400750
C	-5.68581620	-2.15213408	-2.85972481
H	-3.59584575	-1.68460563	-3.03265589
C	-6.91565049	-0.81875832	-1.29238959
H	-5.81365495	0.66726309	-0.25056100
C	-6.86991353	-1.84804314	-2.23765157
H	-5.66089465	-2.94661187	-3.58601351
H	-7.84374852	-0.57576301	-0.80235519
C	-2.26794240	3.16737005	1.20243886
C	-1.09919627	3.86579449	1.53347042
C	-3.45448260	3.49934334	1.80106378
C	-1.14042510	4.87346269	2.46690969
H	-0.17072658	3.61780077	1.05834916
C	-3.49888451	4.51648414	2.75133121
H	-4.34931569	2.97061199	1.53063587
C	-2.35451544	5.19742454	3.08253113

H	-0.24228964	5.40750309	2.71760810
H	-4.43066802	4.77053397	3.22514725
N	-2.39207787	6.27125826	4.09938545
C	-2.13173686	5.69019230	5.43933397
C	-3.20275870	5.23030083	6.21267382
C	-0.61739016	5.06579653	7.19127652
C	-2.97323481	4.69733925	7.45797444
H	-4.20820848	5.28935328	5.83408982
C	-1.66905917	4.61337141	7.95105928
H	0.38614713	4.99961881	7.57301016
H	-3.79795848	4.34336355	8.05026063
H	-1.48571432	4.19928635	8.92572684
C	-1.35614044	7.28399966	3.78577118
C	-0.07352584	7.15358634	4.32436940
C	-1.65379013	8.34809475	2.97016342
C	0.88767672	8.09389255	4.04172221
H	0.16307809	6.31998356	4.96123479
C	-0.67768320	9.30249235	2.68252700
H	-2.64141578	8.44204934	2.55528075
C	0.58345254	9.17637714	3.21496965
H	1.87347577	7.99241537	4.45880615
H	-0.90875467	10.13618208	2.04544698
H	1.33366833	9.91366101	2.99162371
C	-0.85107964	5.60705688	5.92614151

H	-0.03027558	5.95756160	5.32755050
C	0.30718133	2.42305695	-0.02276211
N	1.27315459	3.00153895	0.25992775
C	-0.93313313	0.59168634	-1.27944108
O	0.18570688	0.20497342	-1.68861479
N	-2.08221645	0.00324880	-1.70713532
H	-2.05355177	-0.70561671	-2.43144541
C	-8.15784314	-2.61471873	-2.59128091
N	-9.11676583	-3.18553489	-2.85458254

Output file of **TPA-CNA** (B3LYP/6-311G(d))

C	-3.04013495	0.39847070	-0.27579139
C	-1.69348906	0.37596160	0.10985341
C	-1.11810130	1.50158185	0.71426601
C	-1.90272713	2.63893062	0.89915348
C	-3.24781208	2.62722480	0.48901554
H	-1.10567260	-0.50167681	-0.05204228
C	0.35876496	1.47155160	1.18448735
C	1.13576213	0.31795756	0.92634462
C	0.90807378	2.52798337	1.83697382
C	2.42023429	0.25111989	1.36019802
H	0.69391703	-0.50487198	0.38246826
C	2.24269274	2.45209906	2.30355947
H	0.33477429	3.42830507	2.01237978
C	2.97629529	1.32835580	2.08831035

H	3.02279930	-0.62382162	1.16405123
H	2.66643849	3.29394507	2.83428803
C	-3.65376093	-0.88913498	-0.91859768
C	-2.90150075	-2.01736402	-1.06310098
C	-5.00475680	-0.89160555	-1.34431205
C	-3.47207865	-3.18827283	-1.62196232
H	-1.86461805	-2.03272391	-0.75480057
C	-5.54883224	-2.01656654	-1.88265388
H	-5.59416061	0.00779368	-1.23880561
C	-4.76664131	-3.18925428	-2.01954867
H	-2.86430210	-4.07830280	-1.72633281
H	-6.57882405	-2.02970724	-2.20890733
N	4.36194425	1.23587610	2.61139711
C	4.44311314	1.98252388	3.88257947
C	4.18086237	1.31897720	5.10423978
C	4.76268993	3.30153430	3.88112904
C	4.24467356	2.00194763	6.27546781
H	3.92788625	0.26799523	5.09236688
C	4.82806568	4.01374623	5.10205361
H	4.96705035	3.81895155	2.95369488
C	4.57285704	3.37778924	6.27400153
H	4.04619021	1.50524075	7.21559192
H	5.08052249	5.06489603	5.08857838
H	4.62007465	3.91162892	7.21327507

C	5.32980291	1.79963772	1.64253707
C	5.65286792	3.11880654	1.69188305
C	5.91596142	0.96613008	0.66108144
C	6.57917800	3.65628807	0.76649623
H	5.21128479	3.76788586	2.43627639
C	6.80443407	1.48254391	-0.22677286
H	5.65038632	-0.08096883	0.62911888
C	7.14332451	2.85501021	-0.17247873
H	6.83060356	4.70686102	0.81781916
H	7.26143101	0.85406074	-0.97881777
H	7.85054169	3.25465694	-0.88662655
N	-3.77668903	1.52143604	-0.08306095
C	-1.29418469	3.88957418	1.56391233
N	-0.84114551	4.82058667	2.05878394
O	-4.04914244	3.80326466	0.69767225
C	-5.32514394	3.64807891	0.07079494
H	-5.19808574	3.44046775	-0.97151073
H	-5.83986016	2.83444019	0.53710538
C	-6.15152208	4.94074475	0.23421107
H	-6.25222598	5.17179494	1.27735059
H	-5.65843919	5.74828597	-0.26131348
C	-7.55310921	4.72728987	-0.37006459
H	-8.04145798	3.92338518	0.13630228
H	-7.45787273	4.48914513	-1.41080059

C	-8.38500358	6.01434155	-0.21768269
H	-7.89919225	6.81807195	-0.72685349
H	-9.35860086	5.86138652	-0.63491630
H	-8.47882246	6.25528085	0.82238166
C	-5.40569673	-4.46813858	-2.62502237
N	-5.87545134	-5.41794659	-3.07320066

References

1. Dolomanov, O. V. B.; L. J.; Gildea, R. J.; Howard, J. A.; Puschmann, H. J. A. C., OLEX2: a complete structure solution, refinement and analysis program. *Applied Crystallography* **2009**, *42* (2), 339-341.
2. Sheldrick, G. M. J. C. S. C., Crystal structure refinement with SHELXL. *Crystal Structure Communications* **2015**, *71* (1), 3-8.
3. Sheldrick, G. M. J. F. o. C., SHELXT–Integrated space-group and crystal-structure determination. *Foundations of Crystallography* **2015**, *71* (1), 3-8.
4. Lim, C.; Kim, Y.; Lee, S.; Park, H. H.; Jeon, N. J.; Kim, B. J., Oligo(ethylene glycol)-incorporated hole transporting polymers for efficient and stable inverted perovskite solar cells. *Journal of Materials Chemistry A* **2023**, *11* (12), 6615-6624.
5. Lu, T.; Chen, F., Multiwfn: A multifunctional wavefunction analyzer. *Journal of Computational Chemistry* **2012**, *33* (5), 580-592.
6. Lu, T., A comprehensive electron wavefunction analysis toolbox for chemists, Multiwfn. *The Journal of Chemical Physics* **2024**, *161* (8), 082503.